



Compact modelling-based coupled simulation of RF-MEMS networks for 5G and Internet of Things (IoT) applications

J. Iannacci¹

Received: 4 May 2018 / Accepted: 15 May 2018 / Published online: 21 May 2018
© Springer-Verlag GmbH Germany, part of Springer Nature 2018

Abstract

In this work, the exploitation of an on-purpose software library, previously presented by the author, is discussed in order to simulate the coupled behaviour of RF-MEMS (MicroElectroMechanical-Systems for Radio Frequency applications) devices and networks within a commercial integrated circuits (ICs) development framework. After the validation of the proposed tool against electromechanical experimental measurements of an RF-MEMS switch, the software library is exploited to simulate the multiphysics electromechanical and electromagnetic behaviour of a MEMS-based reconfigurable RF power step attenuator (complex network) manufactured within a surface micromachining RF-MEMS technology platform. The dynamic (transient) electromechanical measured behaviour of the MEMS switches comprised in the attenuator is well-predicted by the simulations based on the implemented compact models, proving the latter ones properly take into account all the salient features determining the coupled behaviour of MEMS devices, i.e. electromechanical transduction, elasticity, inertia, as well as dissipative effects, like gas viscous damping. Furthermore, simulation of the RF-MEMS complex network is completed by the inclusion of S-parameters (Scattering parameters) behaviour. To this purpose, frequency analysis of different attenuation levels realised by the network, depending on the configuration of several micro-switches, is performed. The case study reported in this paper represents a comprehensive exploitation example of the MEMS compact model library, aimed to the coupled electromechanical and electromagnetic simulation of RF-MEMS devices and networks within commercial ICs development tools, like Cadence, Keysight advanced design system (ADS), Mentor, and so on. Eventually, the discussion presented in this paper mentions a rather efficient solution to enable the simulation of entire hybrid circuits and blocks, composed of MEMS/RF-MEMS passive elements and standard semiconductor active circuitry (e.g. CMOS), within the same analysis and development environment.

1 Introduction

MEMS (MicroElectroMechanical-Systems) technology for radio frequency (RF) and Microwave applications, i.e. RF-MEMS, has emerged as a valuable solution to improve performance and reconfigurability of transceivers (transmitters/receivers) in diverse application scenarios, like mobile handsets and smartphones, satellites, surveillance and monitoring systems, and so on (De Los Santos 2002; Varadan 2003). To this regard, the hectic and wide application landscapes of 5G, i.e. the 5th generation of mobile communications and of the Internet of Things (IoT), have recently boosted the attention on the potential of RF-

MEMS technology in order to design and manufacture very-high performance, wideband and frequency agile passive components (Iannacci 2015).

Several of the services we leverage on a daily basis, like WiFi Internet access and video streaming, will be covered by the 5G standard, together with classical functionalities, such as voice calls and Internet on the move access. In addition, machine-to-machine (M2M) communication data are envisaged to travel through 5G (Iannacci 2018a, b; Iannacci 2017). In other words, relevant part of the IoT data traffic will weight on 5G. Many predictions appeal for an enhancement in transmission capacity as huge as 1000 times with respect to 4G-LTE, i.e. the 4th generation Long-Term Evolution, delivering 10 Gb/s to each individual user. Given such premises, it is useful trying to figure out how 5G high-level characteristics will reflect in terms of demands and expected performances of RF passives. Emerging mobile applications will urge for pronounced

✉ J. Iannacci
iannacci@fbk.eu

¹ Center for Materials and Microsystems (CMM), Fondazione Bruno Kessler (FBK), Povo, Trento, Italy

frequency agility and reconfigurability. RF transceivers will have to be agile in aggregating multiple components, working at few GHz (below-6 GHz) as well as up to 60–70 GHz (millimetre-Wave range) (Iannacci et al. 2016a, b, c, 2018a, b). Integrated arrays of antennas and radio frequency front ends (RFFEs) with boosted performance will be necessary, both for increasing multiple input multiple output (MIMO) antennas order, as well as to face the beamforming challenge.

Exploitation of RF-MEMS components, like lumped elements as well as complex networks, always requires hybridisation with control and functional circuitry realised in standard technology, i.e. CMOS. Nonetheless, this consideration poses several issues one has to cope with. On one side, there are several aspects concerning integration and packaging of different (incompatible) technologies (Larcher et al. 2009a, b; Iannacci et al. 2008; Persano et al. 2016; Sordo et al. 2013) as well as reliability and performance stability (Iannacci et al. 2010a; Kuenzig et al. 2012; Tazzoli et al. 2009). On the other hand, modelling and simulation of hybrid RF-MEMS/CMOS functional blocks has also to be properly addressed (Lucyszyn 2010). However, given the different physical domains involved, namely, electromagnetic, fluidic and coupled electromechanical (Hailongk et al. 2006), it would be desirable to have a unique software environment in order to carry out performance optimisation of the whole hybrid block at once.

The scientific community has pursued several approaches in order to address such a relevant issue. On one side, exploitation of finite element method (FEM) tools enables coupling of different physical domains, thus allowing behavioural simulation of MEMS/RF-MEMS. An example concerning the modelling of an RF-MEMS switch within the ANSYS Multiphysics FEM commercial tool is reported in (Malik et al. 2008), while the benchmark of different commercial FEM tools is discussed in (Peyrou et al. 2006). Despite FEM tools make possible to obtain a rather high-level of accuracy, they are not well-suited to address the simulation of an entire sub-system featuring both MEMS passive parts and active control (CMOS) circuitry. To this purpose, approaches based on compact and analytical modelling are proposed in literature (Gaddi et al. 2003; Niessner et al. 2010a). For instance, the simulation of a hybrid RF-MEMS/CMOS voltage controlled oscillator (VCO) is discussed in (Behera et al. 2005). The MEMS part is described by means of analytical models interfaced with active circuitry within a commercial integrated circuit (IC) simulator. Other approaches based on the so-called reduced order modelling (ROM) start from accurate simulation of MEMS/RF-MEMS within (commercial) FEM tools, and then exploit suitable algorithms to reduce the model complexity, making the whole simulation process

manageable within a standard IC simulator. Significant examples related to application of the ROM method to MEMS and RF-MEMS devices are reported in Niessner et al. (2006 and Del Tin et al. 2007).

Bearing in mind the issues discussed thus far, the author already presented an in-house developed MEMS compact model software library, implemented in a standard programming language, within a commercial framework for the simulation and development of ICs (Iannacci et al. 2007). In this work, the mentioned tool is validated by comparison of simulations against measurements of an RF-MEMS ohmic switch. Subsequently, the software library is exploited to simulate the mixed RF/electromechanical behaviour of a complex RF-MEMS network, namely, a multi-state RF power step attenuator, designed, fabricated and tested in the RF-MEMS technology available at the Center for Materials and Microsystems (CMM) of Fondazione Bruno Kessler (FBK) (Iannacci et al. 2009b).

The paper is arranged as follows. After the current Sect. 1 that introduces the frame of reference, the following Sect. 2 discusses the RF-MEMS technology platform employed for the manufacturing of the physical samples analysed in the rest of the work. Section 3 reports the validation of the compact model library capabilities in predicting the coupled electromechanical behaviour of MEMS, by focusing on the case study of an RF-MEMS series ohmic switch. Then, Sect. 4 shows how the mentioned compact modelling approach can be employed in order to simulate the coupled field electromechanical and electromagnetic behaviour of a complex RF-MEMS device, namely a multi-state reconfigurable step power attenuator. Eventually, some conclusive considerations are condensed in Sect. 5.

2 The CMM-FBK RF-MEMS technology

The RF-MEMS technology available at the Center for Materials and Microsystems (CMM) of Fondazione Bruno Kessler (FBK), in Italy, relies on a surface micromachining process based on Gold. High-resistivity Silicon or Quartz 6 inch wafers are employed as starting material. An insulating 1 μm -thick field oxide is grown on top of the substrate and then Boron doped high-resistivity Poly-Silicon layer ($\sim 1.5 \text{ k}\Omega/\text{sq}$) is deposited (630 nm-thick). This material is particularly suitable to implement DC bias lines and electrodes (Gaddi et al. 2004). Poly-Silicon is covered with a 300 nm oxide layer above which an Aluminium based Multi-Metal sandwiched layer is sputtered (630 nm thick). Poly-Silicon and Multi-Metal layers are electrically in contact to each other wherever vias are opened in the intermediate oxide. Elsewhere, such conductive layers enable the implementation of metal insulator metal (MIM)

capacitors. The Multi-Metal is covered with a 100 nm oxide and wherever vias are opened, a 150 nm Gold layer is evaporated in order to ensure optimal Gold-to-Gold ohmic contact with the above layers (still to be mentioned). The surface metallisation consists in a 1.8 μm -thick electroplated Gold layer and air-gaps are obtained wherever such a metal is deposited over a 2–5 μm sacrificial photoresist. In order to get stiffer Gold membranes, a second Gold metallisation (about 3 μm -thick) is electroplated on top of the first one. The suspended Gold membranes enable the implementation of metal air metal (MAM) variable capacitors or ohmic switches, depending on how the bottom electrodes are designed. Figure 1 reports a 3D schematic of a series ohmic cantilever (i.e. a single hinged membrane) realised in the CMM-FBK RF-MEMS surface micromachining technology.

The Poly-Silicon electrode underneath the suspended Gold membrane is visible. It is needed for DC biasing of the cantilever switch that, after pull-in is reached (namely the collapse onto the underneath electrode) (Giacomozzi et al. 2011), establishes an ohmic contact with the underneath Gold layer, closing, in turn, the electrical contact between the input and output terminations (CLOSED switch).

3 Experimental validation of the MEMS compact models

In this section, the accuracy of the implemented models is verified by comparing the simulated electromechanical behaviour of an RF-MEMS switch against experimental data. Figure 2 reports the 3D profile of a series ohmic switch, obtained with a white light profiling system based on optical interferometry (Iannacci et al. 2009b). The

suspended switch is formed by a thick Gold central plate (see Sect. 2 describing the employed technology) connected to four straight suspensions, as reported in the close-up visible in the top image in Fig. 2.

The central plate dimensions are 260 and 140 μm along the X- and Y-axis, respectively. Moreover, 15 holes (20 by 20 μm , spaced 20 μm from each other and from plate edges) are opened on the membrane, in order to allow proper removal of the underlying sacrificial layer and release of the suspended structure. Finally, the straight beams length, width and thickness are 165, 10 and 1.8 μm , respectively. The micro-relay is framed within a Coplanar Waveguide (CPW) structure configured for ground-signal-ground (GSG) probing. Furthermore, Gold pad needed to bias the buried Poly-Silicon electrodes underneath the suspended membrane is also visible in Fig. 2.

The electromechanical behaviour of the discussed switch is studied exploiting a MEMS compact model library previously developed leveraging the VerilogA programming language, within the Cadence ICs development framework (Iannacci et al. 2009a). Two relevant electromechanical components are available in the library, namely, a suspended rigid plate, defining variable air-gaps, and a flexible straight beam, in order to implement deformable suspensions. Their proper interconnection at schematic level leads to the composition of complete MEMS devices topologies. The library also includes anchors, for the definition of mechanical constraints, and stimulus sources, like forces and displacements. Quantities belonging to different physical domains, i.e. electrical and mechanical, are easily handled by the simulator. According to the Kirchhoff's laws, such magnitudes are managed as *through quantities* (e.g. electrical currents and mechanical forces) and *across quantities* (e.g. voltages and mechanical displacements). The schematic of the switch in Fig. 2, built

Fig. 1 3D schematic view of a series ohmic cantilever switch manufactured in the CMM-FBK RF-MEMS technology. The Poly-Silicon electrode for DC biasing is visible as well as the Gold contact underneath the suspended cantilever free end

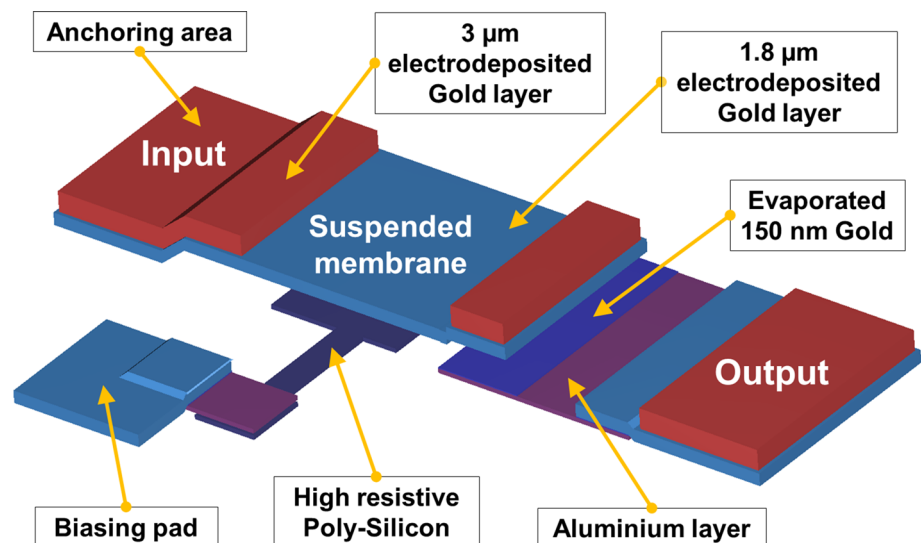


Fig. 2 3D measured profile of a MEMS series ohmic switch sample fabricated in the CMM-FBK RF-MEMS technology (bottom image). The device is based on a central Gold plate connected to four straight flexible suspensions. The close-up (top image) shows the 2D view of the central plate, straight suspensions and anchors

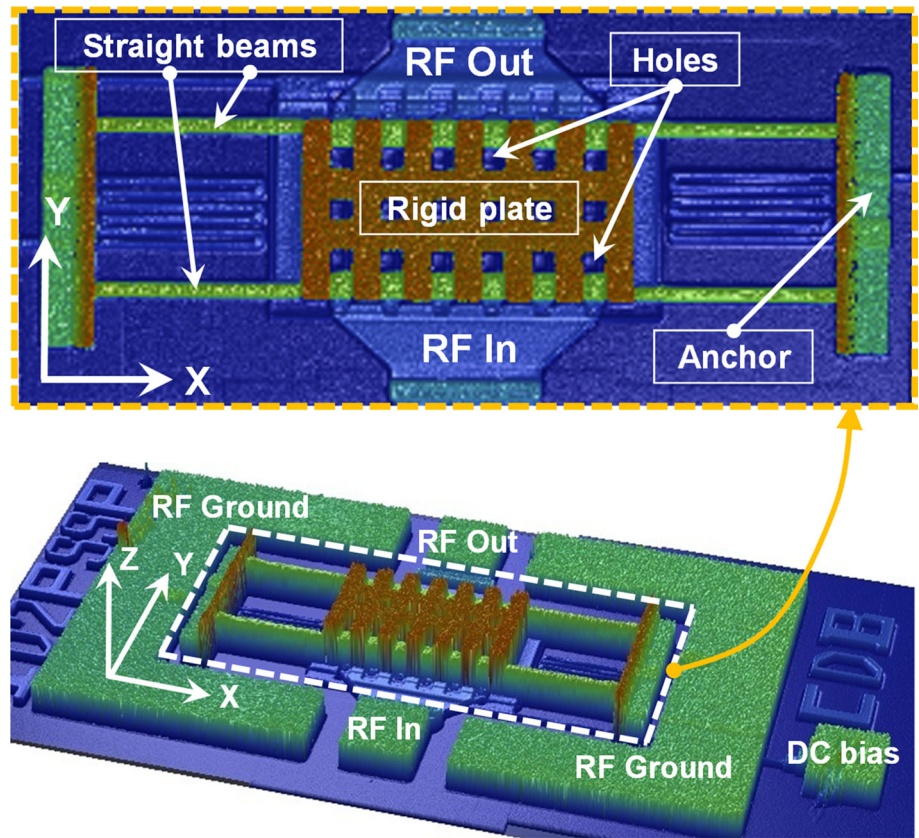
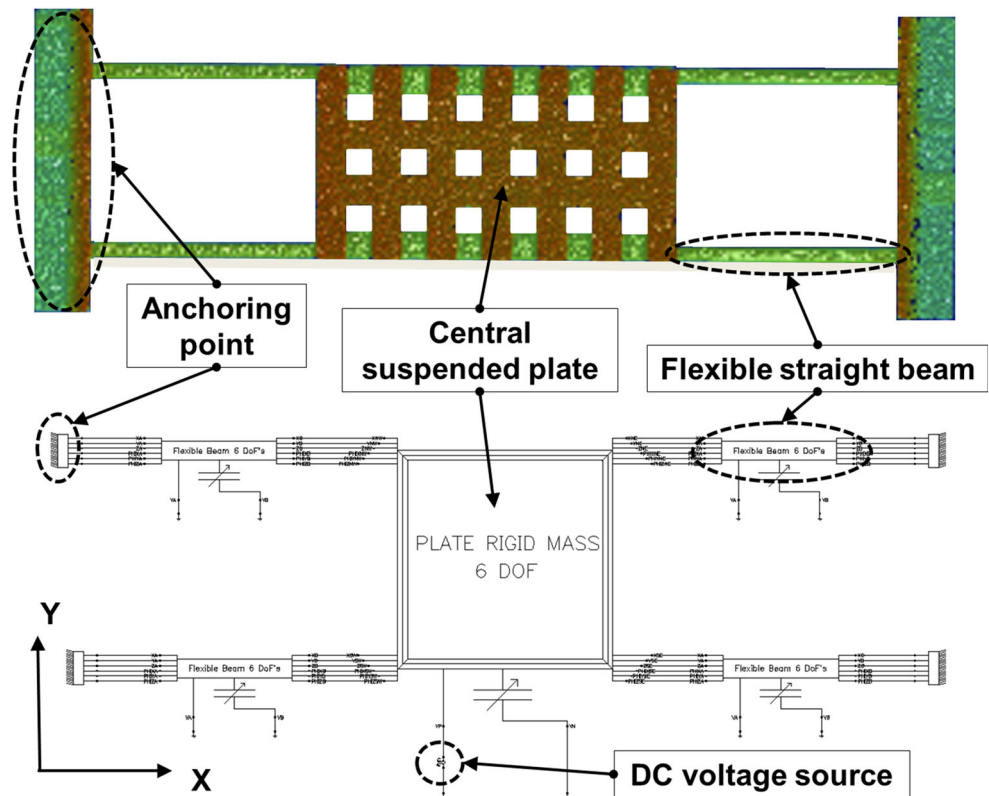


Fig. 3 Schematic (bottom image) of the MEMS ohmic switch reported in Fig. 2 implemented with the elementary MEMS components available in the compact model library exploited to perform electromechanical simulations. The correspondence with the physical MEMS device (top image) is highlighted



with the elementary components available in the library, is reported in Fig. 3.

Correspondence between the physical suspended MEMS bridge (Fig. 3-top) and the simulation schematic (Fig. 3-bottom) is highlighted. Coupled electromechanical behaviour of the RF-MEMS switch is simulated in dynamic conditions and compared against experimental data. This way, the overall switch physical characteristics described by compact models, i.e. mechanical deformations, inertia, viscous damping and electromechanical coupling, are validated at once (Niessner et al. 2010b, 2011, 2012). The experimental dynamic characteristic of the switch depicted in Fig. 2 is acquired by means of the same profiling system mentioned above, but using a stroboscopic (pulsed) light instead of continuous white light, in order to capture the switch vertical displacement for various bias levels imposed (Novak et al. 2003). The applied voltage is a 500 Hz square pulse (50% duty-cycle) with ON/OFF levels of 33 V and 0 V, respectively. The measured pull-in (actuation) voltage of the switch, previously observed in static conditions and not detailed in any plot here, is 32 V, while the pull-out (release) voltage is 24 V. This means the pulse ON level is large enough to bring RF-MEMS switch to actuation in dynamic conditions. On the other hand, the switch schematic reported in Fig. 3-bottom is simulated (transient simulation) applying a voltage pulse with the same characteristics just discussed concerning experiments. The comparison of the measured and simulated dynamic characteristic of the RF-MEMS switch is reported in Fig. 4. The curves well compare to each other, proving the compact models implemented in VerilogA accurately capture the main physical characteristics of the RF-MEMS micro-relay.

The close-up of the transient characteristic within the 0–100 μs interval is reported in Fig. 5. The first contact of

the membrane with the underlying fixed electrode takes place in about 30 μs (measurement), despite some bounces impair to reach a stable contact up to 100 μs .

The simulated characteristic underestimates the switch closing time, the first contact being visible after 20 μs . However, the dynamic characteristic of a MEMS switch is quite complex to be properly predicted, given different physical aspects involved in it, and the mentioned disagreement can be accepted at this validation stage. The reached accuracy is also visible in the close-up in Fig. 6, where the measured and simulated release phase is shown.

Ringings of the MEMS switch, as acquired by the optical profiler, is precisely reproduced by the transient simulation. This proves the accuracy of the implemented models, as the frequency and amplitude of oscillations are strictly related to the elastic and inertial characteristics of the MEMS device, while their time evolution is determined by dissipative effects, the squeeze film damping due to the air viscosity being the dominant one in this particular case. Measurements and simulations were performed at ambient temperature and pressure.

The MEMS compact model library discussed in this work has also been validated and utilised concerning prediction of the RF behaviour (S-parameter simulations) (Iannacci et al. 2010b), and not reported here for the sake of brevity. In this case, a suitable lumped element network is wrapped around the intrinsic RF-MEMS device in order to account for all the parasitic effects, like capacitive and resistive coupling to ground, series inductance of input/output sections, and so on. The network topology is defined according to a methodology well-known in microwave transistor modelling (Dambrine et al. 1988).

Fig. 4 Experimental vs. simulated dynamic response of the RF-MEMS switch depicted in Fig. 2 to a 500 Hz, 0–33 V, 50% duty-cycle square pulse. The curves well compare to each other, proving that the main physical characteristics of the switch are properly accounted by the compact models implemented in VerilogA

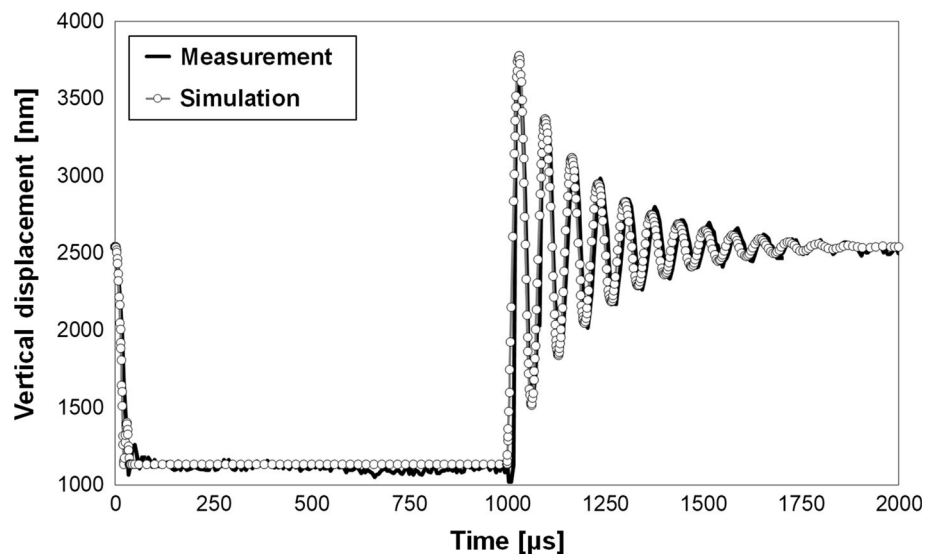


Fig. 5 Close-up of the switch actuation transient in response to the 0 to 33 V transition of the applied square pulse. The first measured contact takes place after about 30 μs , while the simulation underestimates of about 10 μs such a time. Bounces are visible both in the measurement and simulation

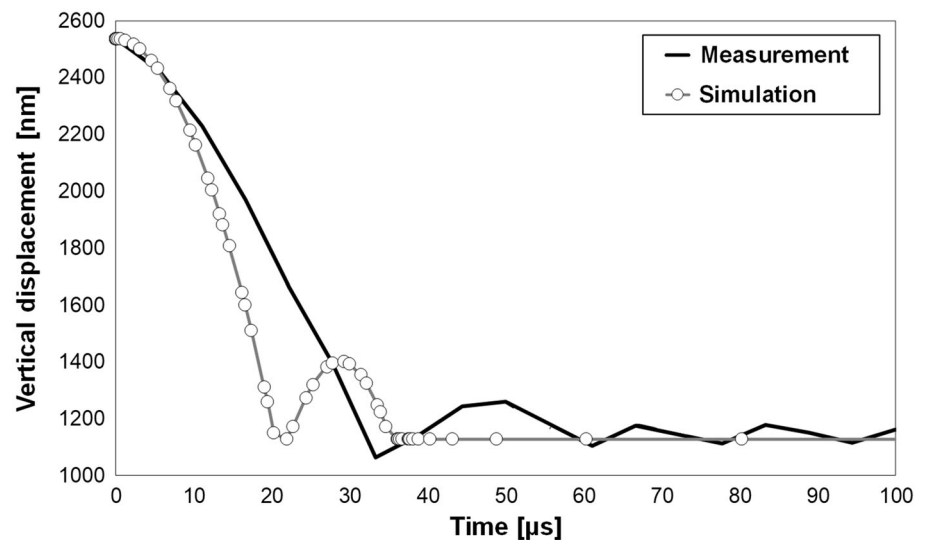
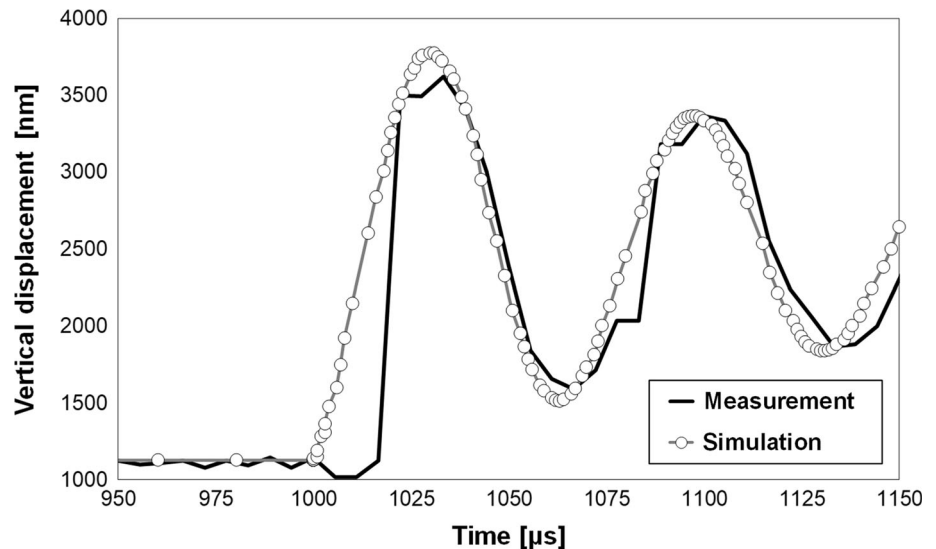


Fig. 6 Close-up of the switch release transient in response to the 33 to 0 V transition of the applied square pulse. Oscillations of the movable MEMS membrane damped because of air viscosity are well predicted by transient simulation



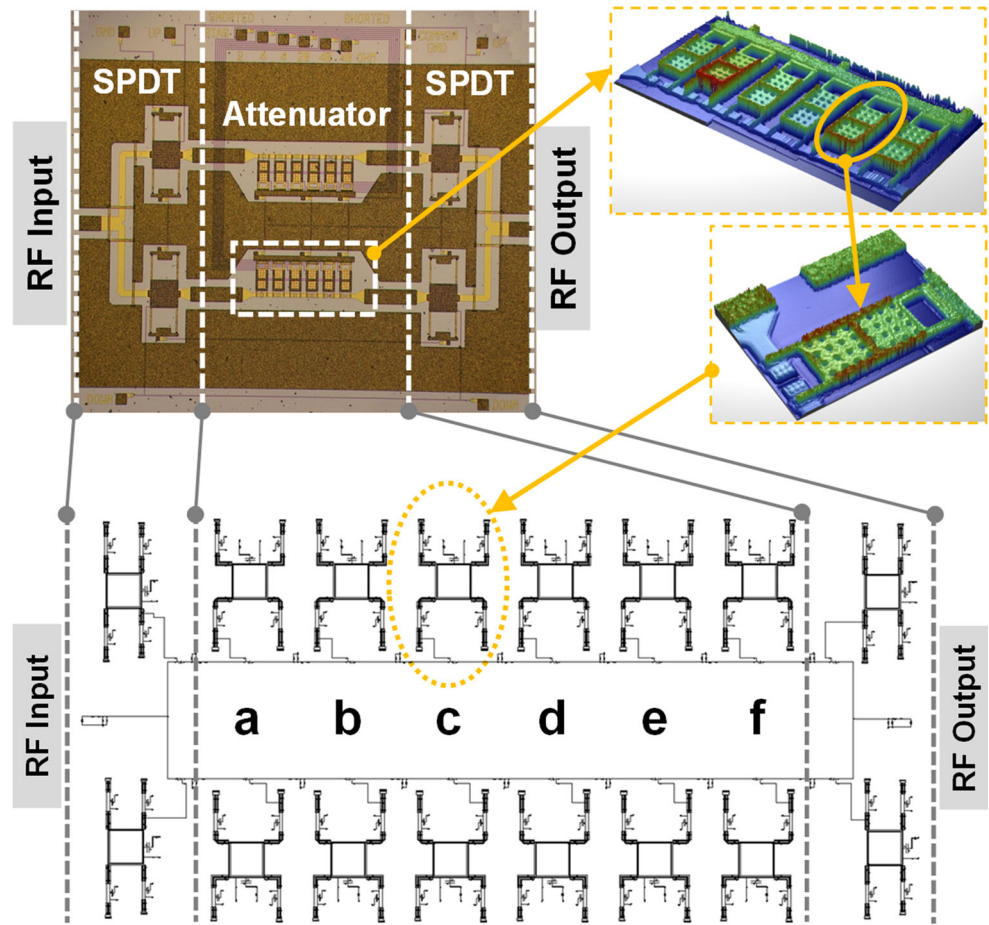
4 Simulation of a reconfigurable MEMS-based RF power attenuator

The MEMS compact model library validated in the previous section is now going to be exploited for the coupled electromechanical and electromagnetic simulation of a complex RF-MEMS-based network. Such a device is a reconfigurable multi-state RF power step attenuator already presented in (Iannacci et al. 2009b). The power attenuator is based on two parallel branches with 6 Poly-Silicon series resistors of different values. Each resistor can be selected or shorted depending on the state (actuated or not actuated) of electrostatically controlled suspended Gold membranes (Iannacci et al. 2010a). Moreover, one or both branches are selected by means of Single Pole Double Throws (SPDTs) based on clamped-clamped MEMS series ohmic switches. Figure 7-top shows a microphotograph of the fabricated

network together with a close-up (3D profilometer) of one branch and one single MEMS suspended membrane.

The whole network is implemented with the compact models available in the afore-mentioned MEMS model library, and the schematic is reported in Fig. 7-bottom (Iannacci 2013a, b). The correspondence between the subsections of the physical network and the schematic are highlighted in figure, and the 6 resistive loads are labelled with letters from “a” to “f”. Each cantilever-type RF-MEMS switch (selecting or shorting each Poly-Silicon resistor) is composed with the elements available in the VerilogA library. In Fig. 7-top-right the 3D measured profile of a bank of 6 switches comprised in the network, as well as the close-up of a single switch, are visible. In particular, the correspondence between the 3D topology of a single RF-MEMS switch and the simulation schematic is

Fig. 7 Top image. Microphotograph of the entire fabricated RF power attenuator and close-up (obtained with a 3D profilometer based on optical interferometry) of one branch and one single MEMS suspended membrane. Bottom image. Schematic of the entire network assembled with the MEMS compact models implemented in VerilogA. The correspondence between the sub-sections of the physical network and the schematic is highlighted in figure, and the 6 resistive loads are labelled with letters from “a” to “f”



also shown (see section “b”). The measured values of the Poly-Silicon resistors are reported in Table 1.

Each switch in the schematic is connected to a two-state resistor inserted in series along the input/output RF line (Niessner et al. 2011). Such variable resistors assume the values reported in Table 1 when the corresponding RF-MEMS switch is in the rest position, while drop to a low-value (few Ohms) when the switch is actuated. In the latter case, the Poly-Silicon resistor is shorted and the low-resistance value accounts for the ohmic contact of the MEMS switch with the bottom electrodes. The simulation schematic of the whole RF power attenuator is completed by lumped element networks in input and output, accounting for technology non-idealities occurring in correspondence with the Gold to Multi-Metal transitions. Such an unwanted

behaviour is described in (Iannacci et al. 2010a) while the technique for the extraction of the lumped element networks is discussed in (Iannacci et al. 2009a).

The schematic in Fig. 7-bottom is set for S-parameter simulations. The coupled electromechanical and electromagnetic coupling is investigated in two ways. In the first case, the frequency of the simulation is swept from DC up to 40 GHz, as reported in Fig. 8 (S21 transmission parameter).

Parametric simulation is set and the DC bias, applied to the RF-MEMS switches selecting or shorting Poly-Silicon resistors, is allowed to equal 0 or 20 V. In the latter case, the DC bias is larger than the pull-in level (measured and simulated around 13 V), and the corresponding resistive load is shorted. Figure 8 reports a few attenuation levels falling between the maximum one, reached when none of the switches is actuated, and the minimum one, when all the RF-MEMS switches are actuated.

The second way to perform coupled electromechanical and RF simulations is reported in Fig. 9. In this case, S-parameter simulation is performed at 20 GHz, while bias voltage is swept from 0 V up to 20 V, and is applied to each of the micro-relays (from “a” to “f”) one at a time.

Table 1 Measured resistance of the 6 Poly-Silicon resistive loads comprised in the MEMS reconfigurable RF power attenuator

	Resistor label					
	a	b	c	d	e	f
Resistance (Ω)	9.3	18.6	18.6	93	206	206

Fig. 8 S-parameter simulation (S_{21} transmission parameter) of the RF-MEMS power attenuator. The frequency is swept from DC up to 40 GHz and different switch/switches is/are actuated (by applying 20 V DC bias, i.e. above pull-in) to change the attenuation level implemented by the network

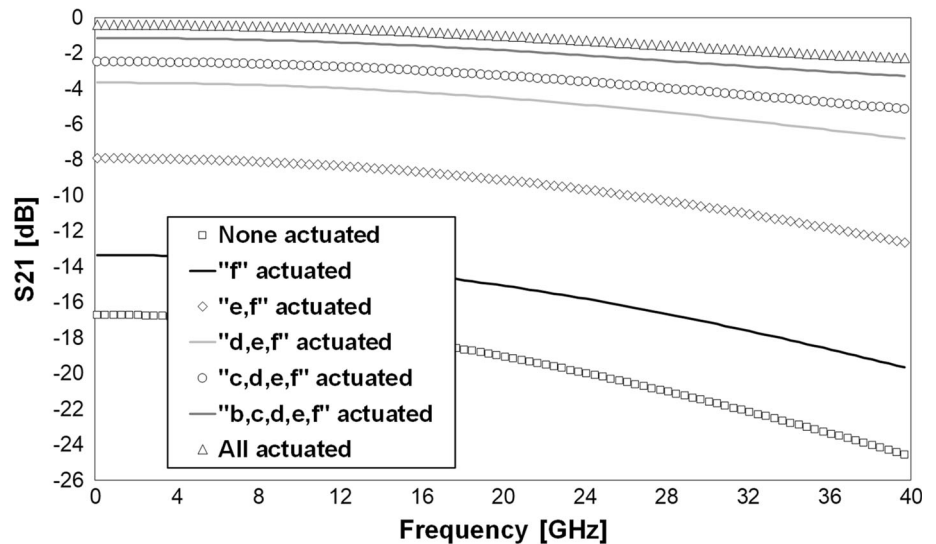
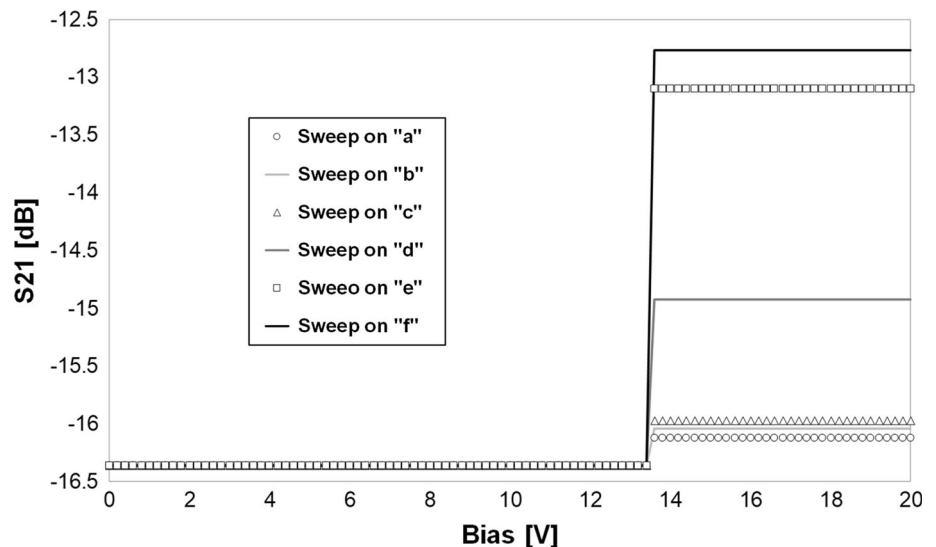


Fig. 9 S-parameter simulation (S_{21} parameter) of the RF-MEMS power attenuator. The frequency is fixed to 20 GHz, while the DC bias is swept from 0 V up to 20 V



This type of analysis makes possible observing the effect of pull-in on the S-parameters behaviour of the whole network. Below pull-in, the attenuation level reported in Fig. 9 (S_{21} parameter) is the largest realised by the network. Differently, after pull-in occurs (at around 13.5 V) the decrease in attenuation depends on the value of the shorted resistor. As final remark, it should be noted that all the discussed simulations required a rather limited time to be completed on a standard PC (from 20 to 50 s up to a few minutes, depending on the complexity of the simulation and of the structure), confirming that the developed MEMS software library represents a fast simulation and optimisation tool.

5 Conclusion

The exploitation of a MEMS compact model software library, previously developed and presented, for the simulation of the mixed RF/electromechanical behaviour of RF-MEMS devices and complex networks was discussed. The attention was dragged at first on the validation of the tool, with reference to the electromechanical behaviour of an RF-MEMS ohmic switch fabricated within a surface micromachining process. Subsequently, the tool was utilised for the RF/electromechanical simulation of a complex network, namely, a reconfigurable RF power programmable step attenuator. The reported simulation methodology allowed obtaining accurate results by keeping the simulation time rather limited. The case study of an RF-MEMS complex network discussed in this paper represents a comprehensive exploitation example of the compact

model library, aimed to the coupled electromechanical and electromagnetic simulation of RF-MEMS devices and networks within commercial Integrated Circuits (ICs) development frameworks.

From the point of view of applications, the hectic and wide application landscapes of 5G, i.e. the 5th generation of mobile communications and of the Internet of Things (IoT), have recently boosted the attention on the potential of RF-MEMS technology in order to design and manufacture very-high performance, wideband and frequency agile passive components. Therefore, availability of comprehensive development environments enabling fast multi-physical optimisation of complex RF-MEMS devices, possibly integrated with semiconductor components within a unique sub-system, becomes of critical importance.

In conclusion, the discussion presented in this paper illustrates a rather efficient solution in order to enable the simulation of entire hybrid circuits, blocks and sub-systems, composed of MEMS/RF-MEMS passive elements and standard semiconductor active circuitry (e.g. CMOS), within a unique analysis and development environment.

References

- Behera M, Kratyuk V, De SK, Aluru NR, Hu Y, Mayaram K (2005) Accurate simulation of RF MEMS VCO performance including phase noise. *IEEE JMEMS* 14:313–325. <https://doi.org/10.1109/JMEMS.2004.839317>
- Dambrine G, Cappy A, Heliodore F, Playez E (1988) A new method for determining the FET small-signal equivalent circuit. *IEEE T-MTT* 36:1151–1159. <https://doi.org/10.1109/22.3650>
- De Los Santos HJ (2002) RF Mems circuit design for wireless communications. Artech House, Norwood
- Del Tin L, Iannacci J, Gaddi R, Gnudi A, Rudnyi EB, Greiner A, Korvink JG (2007) Non linear compact modeling of RE-MEMS switches by means of model order reduction. In: Proceedings of IEEE TRANSDUCERS, pp. 635–638. <https://doi.org/10.1109/sensor.2007.4300210>
- Gaddi R, Iannacci J, Gnudi A (2003) Mixed-domain simulation of intermodulation in RF-MEMS capacitive shunt switches. In: Proceedings of the 33rd European microwave conference, EuMC vol. 2, pp. 671–674. <https://doi.org/10.1109/eumc.2003.177566>
- Gaddi R, Bellei M, Gnudi A, Margesin B, Giacomozzi F (2004) Interdigitated low-loss ohmic RF MEMS switches. In: Proceedings of NSTI nanotechnology, pp. 327–330
- Giacomozzi F, Mulloni V, Colpo S, Iannacci J, Margesin B, Faes A (2011) A Flexible Fabrication Process for RF MEMS Devices. *Rom J Inf Sci Technol ROMJIST* 14:259–268
- Hailongk W, Guangbao S, Youbao L (2006) Lumped behavioral modeling for suspended MEMS. In: Proceedings of the 8th international conference on solid-state and integrated circuit technology ICSICT, pp. 679–681. <https://doi.org/10.1109/icsict.2006.306435>
- Iannacci J (2013a) Practical guide to RF-MEMS. Wiley-VCH, Weinheim
- Iannacci J (2013b) Compact Modeling of RF MEMS devices. In: Brand O, Fedder GK, Hierold C, Korvink JG, Tabata O (eds) System-level modeling of MEMS. Wiley-VCH, Weinheim. <https://doi.org/10.1002/9783527647132.ch8>
- Iannacci J (2015) RF-MEMS: an enabling technology for modern wireless systems bearing a market potential still not fully displayed. *Springer Microsyst Technol* 21:2039–2052. <https://doi.org/10.1007/s00542-015-2665-6>
- Iannacci J (2017) RF-MEMS Technology for High-Performance Passives: The challenge of 5G mobile applications. IOP Publishing, Bristol. <https://doi.org/10.1088/978-0-7503-1545-6>
- Iannacci J (2018a) Internet of things (IoT); internet of everything (IoE); tactile internet; 5G—A (not so evanescent) unifying vision empowered by EH-MEMS (energy harvesting MEMS) and RF-MEMS (radio frequency MEMS). *Elsevier Sens Actuators A Phys* 272:187–198. <https://doi.org/10.1016/j.sna.2018.01.038>
- Iannacci J (2018b) Surfing the hype curve of RF-MEMS passive components: towards the 5th generation (5G) of mobile networks. *Springer Microsyst Technol*. <https://doi.org/10.1007/s00542-018-3718-4>
- Iannacci J, Gaddi R, Gnudi A (2007) Non-linear electromechanical RF model of a MEMS varactor based on VerilogA© and lumped-element parasitic network. In: Proceedings of EUMC 1342–1345. <https://doi.org/10.1109/eumc.2007.4405451>
- Iannacci J, Bartek M, Tian J, Gaddi R, Gnudi A (2008) Electromagnetic optimization of an RF-MEMS wafer-level package. *Elsevier Sens Actuators A Phys* 142:434–441. <https://doi.org/10.1016/j.sna.2007.08.018>
- Iannacci J, Giacomozzi F, Colpo S, Margesin B, Bartek M (2009a) A general purpose reconfigurable MEMS-based attenuator for RF and microwave applications. In: Proceedings of IEEE EUROCON, pp. 1201–1209. <https://doi.org/10.1109/eurcon.2009.5167788>
- Iannacci J, Repchankova A, Macii D, Niessner M (2009b) A measurement procedure of technology-related model parameters for enhanced RF-MEMS design. In: Proceedings of IEEE AMUEM, pp. 44–49. <https://doi.org/10.1109/amuem.2009.5207609>
- Iannacci J, Repchankova A, Faes A, Tazzoli A, Meneghesso G, Dalla Betta G-F (2010a) Enhancement of RF-MEMS switch reliability through an active anti-stiction heat-based mechanism. *Elsevier Microelectron Reliab* 50:1599–1603. <https://doi.org/10.1016/j.microrel.2010.07.108>
- Iannacci J, Gaddi R, Gnudi A (2010b) Experimental validation of mixed electromechanical and electromagnetic modeling of RF-MEMS devices within a standard IC simulation environment. *IEEE JMEMS* 19:526–537. <https://doi.org/10.1109/JMEMS.2010.2048417>
- Iannacci J, Huhn M, Tschoban C, Potter H (2016a) RF-MEMS technology for 5G: series and shunt attenuator modules demonstrated up to 110 GHz. *IEEE Electron Device Lett* 37:1336–1339. <https://doi.org/10.1109/LED.2016.2604426>
- Iannacci J, Huhn M, Tschoban C, Pötter H (2016b) RF-MEMS technology for future (5G) mobile and high-frequency applications: reconfigurable 8-Bit power attenuator tested up to 110 GHz. *IEEE Electron Device Lett* 37:1646–1649. <https://doi.org/10.1109/LED.2016.2623328>
- Iannacci J, Tschoban C, Reyes J, Maaß U, Huhn M, Ndiip I, Pötter H (2016c) RF-MEMS for 5G mobile communications: a basic attenuator module demonstrated up to 50 GHz. In: Proceedings of IEEE SENSORS, pp. 1–3. <https://doi.org/10.1109/sensors.2016.7808547>
- Kuenzig T, Iannacci J, Schrag G, Wachutka G (2012) Study of an active thermal recovery mechanism for an electrostatically actuated RF-MEMS switch. In: Proceedings of IEEE EuroSime, pp. 1–7. <https://doi.org/10.1109/esime.2012.6191766>

- Larcher L, Brama R, Ganzerli M, Iannacci J, Margesin B, Bedani M, Gnudi A (2009) A MEMS reconfigurable quad-band class-E power amplifier for GSM standard. In: Proceedings of IEEE MEMS, pp. 864–867. <https://doi.org/10.1109/memsys.2009.4805520>
- Larcher L, Brama R, Ganzerli M, Iannacci J, Bedani M, Gnudi A (2009) A MEMS reconfigurable quad-band class-E power amplifier for GSM standard. In: Proceedings of IEEE DATE, pp. 364–368. <https://doi.org/10.1109/date.2009.5090689>
- Lucyszyn S (2010) Advanced RF MEMS. Cambridge University Press, Cambridge
- Malik AF, Shoaib M, Naseem S, Riaz S (2008) Modeling and designing of RF MEMS switch using ANSYS. In: Proceedings of the 4th international conference on emerging technologies ICET, pp. 44–49. <https://doi.org/10.1109/icet.2008.4777472>
- Niessner M, Schrag G, Wachutka G (2006) Extraction of physically based high-level models for rapid prototyping of MEMS devices and control circuitry. In: Proceedings of IEEE SENSORS, pp. 915–918. <https://doi.org/10.1109/icsens.2007.355615>
- Niessner M, Schrag G, Wachutka G, Iannacci J (2010) Modeling and fast simulation of RF-MEMS switches within standard IC design frameworks. In: Proceedings of SISPAD, pp. 317–320. <https://doi.org/10.1109/sispad.2010.5604496>
- Niessner M, Iannacci J, Peller A, Schrag G, Wachutka G (2010) Macromodel-based simulation and measurement of the dynamic pull-in of viscously damped RF-MEMS switches. In: Proceedings of eurosensors XXIV conference, pp. 78–81. <https://doi.org/10.1016/j.proeng.2010.09.052>
- Niessner M, Schrag G, Iannacci J, Wachutka G (2011) Macromodel-based simulation and measurement of the dynamic pull-in of viscously damped RF-MEMS switches. Elsevier Sens Actuators A Phys 172:269–279. <https://doi.org/10.1016/j.sna.2011.04.046>
- Niessner M, Schrag G, Iannacci J, Wachutka G (2012) Squeeze-film damping in perforated microstructures: modeling, simulation and pressure-dependent experimental validation. In: Proceedings of microtech conference, pp. 598–601
- Novak E, Wan, D-S, Unruh P, Schurig M (2003) MEMS metrology using a strobed interferometric system. In: Proceedings IMEKO, pp. 178–182. <https://doi.org/10.1109/icmens.2003.1222010>
- Persano A, Siciliano P, Quaranta F, Lucibello A, Marcelli R, Capoccia G, Proietti E, Bagolini A, Iannacci J (2016) Wafer-level thin film micropackaging for RF MEMS applications. In: Proceedings of DTIP, pp. 1–5. <https://doi.org/10.1109/dtip.2016.7514826>
- Peyrou D, Pons P, Granier H, Leray D, Ferrand A, Yacine K, Saadaoui M, Nicolas A, Tao JW, Plana R (2006) Multiphysics softwares benchmark on ansys/comsol applied For RF MEMS switches packaging simulations. In: Proceedings of EuroSime, pp. 1–8. <https://doi.org/10.1109/esime.2006.1644011>
- Sordo G, Faes A, Resta G, Iannacci J (2013) Characterization of quartz-based packaging for RF-MEMS. Proc SPIE 8763:1–9. <https://doi.org/10.1117/12.2017856>
- Tazzoli A, Autizi E, Barbato M, Meneghesso G, Solazzi F, Farinelli P, Giacomozzi F, Iannacci J, Margesin B, Sorrentino R (2009) Evolution of electrical parameters of dielectric-less ohmic RF-MEMS switches during continuous actuation stress. In: Proceedings of ESSDERC 2009, pp. 343–346. <https://doi.org/10.1109/essderc.2009.5331307>
- Varadan VK (2003) RF Mems & their applications. Wiley, Hoboken

Publisher's Note Springer Nature remains neutral with regard to jurisdictional claims in published maps and institutional affiliations.